Available online at www.sciencedirect.com
SCIENCE DIRECT®
Journal of Chromatography B, 808 (2004) 295–302
JOURNAL OF CHROMATOGRAPHY B
www.elsevier.com/locate/chromb

Subcellular metabolite profiles of the parent CCRF-CEM and the derived CEM/C2 cell lines after treatment with doxorubicin

Adrian B. Anderson, Edgar A. Arriaga*

Department of Chemistry, University of Minnesota, 207 Pleasant Street SE, Minneapolis, MN 55455, USA

Received 7 January 2004; received in revised form 17 May 2004; accepted 18 May 2004

Available online 20 June 2004

Abstract

Micellar electrokinetic capillary chromatography with laser-induced fluorescence detection was used to detect the differences in doxorubicin metabolite accumulation in four subcellular fractions isolated from the CCRF-CEM and the CEM/C2 human leukemia cell lines. Five fluorescent metabolites and doxorubicin make up the metabolite profile of these cell lines upon treatment with 10 μM doxorubicin for 12 h, cell lysis, and fractionation by differential centrifugation. Based on the relative electrophoretic mobility of synthetic standards, we tentatively identify one metabolite as 7-deoxydoxorubicinone and suggest that doxorubicinone is not among those metabolites detected. Although the obvious difference between the derived cell line (CEM/C2) and the parent cell line (CCRF-CEM) is the decreased topoisomerase I activity in the former, the results presented here indicate that each cell line has a unique distribution of metabolites in each one of four subcellular fractions: nuclear-enriched, heavy-organelle-enriched, light-organelle-enriched, and cytoplasmic fractions.

Keywords: Metabolism; Micellar electrokinetic capillary chromatography; Doxorubicin

1. Introduction

While doxorubicin (DOX) has been proven effective against a wide variety of neoplasms [1,2], its clinical utility has been limited by the development of serious side effects, most notably irreversible cardiotoxicity [3–6]. Since DOX undergoes metabolic transformations within the cell [6], these side effects may not be necessarily directly associated with DOX, but with DOX metabolites. The determination of DOX metabolites within specific subcellular environments may therefore help us understand the links between DOX metabolism, efficacy, and cytotoxicity. For example, metabolites found in the nucleus, where DOX has been reported to interact with DNA and the enzyme topoisomerase IIα [7,8], may be related to the efficacy of DOX treatment. Metabolites found in mitochondria, such as DOX aglycones [5,9–14], have been reported to increase Ca^{+2}-dependent inner mitochondrial membrane permeability and modify this organelle's sulfhydryl groups [5]. Metabolites that accumulate in the mitochondria are likely involved in cytotoxicity. Because DOX accumulates in acidic organelles and this accumulation has been linked to drug resistance [15], it is speculated that metabolites also accumulate in these organelles and affect drug resistance.

With the exception of doxorubicinol, the most abundant DOX metabolite [16–18], DOX metabolites are very low in abundance (i.e. <1% of the DOX concentration) [19]. Despite their low abundance, those DOX metabolites that preserve the native fluorescence of DOX have been successfully detected with sensitive laser-induced fluorescence (LIF) [19–21]. Using capillary electrophoresis (CE) with LIF detection, Simeon et al have detected sub-nanomolar DOX concentrations [21], and we have previously used micellar electrokinetic capillary chromatography (MEKC) with LIF detection to analyze sub-attomole amounts of as many as eleven metabolites produced in cultured NS-1 mouse hybridoma cells [19–21]. The latter can also be used to study the subcellular accumulation of DOX metabolites in subcellular fractions prepared from NS-1 cell lysates [20].

Here we report on the use of MEKC with LIF detection to separate metabolites and create subcellular metabolite pro-

* Corresponding author. Tel.: +1 612 624 8024; fax: +1 612 626 7541.
E-mail address: arriaga@chem.umn.edu (E.A. Arriaga).

1570-0232/$ – see front matter © 2004 Elsevier B.V. All rights reserved.
doi:10.1016/j.jchromb.2004.05.017

files for two leukemia cell lines: CCRF-CEM and CEM/C2. The latter was isolated by chronically treating CCRF-CEM with camptothecin [22] which targets the catalytic site of topoisomerase I [23]. Although it was expected that a single mutation in topoisomerase I, a non-target for DOX, would not trigger DOX cross-resistance or alter DOX metabolism directly, our analysis of subcellular fractions by MEKC with LIF detection shows that CCRF-CEM and CEM/C2 are metabolically different. Most importantly, one of the tentatively identified metabolites, 7-deoxydoxorubicinone (7-deoxyDOXone), which is associated with cytotoxicity, was found to be more abundant in the CCRF-CEM subcellular fractions than in the fractions of the other cell line. On the other hand, another expected metabolite, doxorubicinone (DOXone), was found to be absent from all the subcellular fractions in both cell lines.

2. Experimental

2.1. Chemicals and reagents

DOX and doxorubicinol were donated by Dr. A. Suarato (Pharmacia, Nerviano, Italy). DOXone and and 7-deoxyDOXone were purchased from Qvantas, Inc. (Newark, DE, USA). Sodium borate decahydrate was purchased from EM Science (Gibbstown, NJ, USA). Sodium dodecyl sulfate (S.D.S) Ultrapure Bioreagent was obtained from J. T. Baker (Phillipsburg, NJ, USA). Methanol (MeOH) and sucrose were purchased from Mallinckrodt (Paris, KY, USA). Tris-HCl, ethylenediaminetetraacetic acid (EDTA), Phosphate buffered saline (PBS), and tryptan blue solution were purchased from Sigma (St. Louis, MO, USA). Phenylmethylsulfonyl fluoride (PMSF) was purchased from Calbiochem (San Diego, CA, USA). MEKC buffer was 10 mM borate, 10 mM S.D.S (pH 9.4) (BS buffer). Cell washing and suspension was done with either PBS or 200 mM sucrose, 10 mM Tris-HCl, 0.1 mM EDTA, 97 μM PMSF (pH 7.4) (STEP buffer). All buffers were made using 18 MΩ water obtained from a Millipore water purification system (Millipore, Billerica, MA) that had been filtered through a 0.22 μm Nalgene filter and stored at room temperature for up to one month. The pH of all solutions was adjusted with either HCl or NaOH. Following pH adjustment, buffers were filtered through a 0.22 μm Nalgene filter and stored at room temperature for up to one month.

Stock solutions of DOX and metabolites were prepared in 100% MeOH at the following concentrations: 3.0×10^{-3} M DOX; 1.7×10^{-3} M doxorubicinol; 1.0×10^{-3} M DOXone; 1.0×10^{-3} M 7-deoxyDOXone. The stock solutions were stored at −20 °C and used up to a month post preparation. On the day of analysis a working solution for each analyte was prepared in BS buffer to prevent repeated freeze/thaw cycling of the entire stock solution between −20 °C and 25 °C.

2.2. Cell culture

CEM/C2 and CCRF-CEM cells (purchased from American Type Culture Collection (ATCC) (Manassas, VA, USA)) were cultured at 37 °C and 5% CO_2 in RPMI 1640 media (ATCC). Thirty hours after splitting, cells were treated with 10 μM DOX for 12 h. Trypan Blue Solution (0.4%) was used to stain non-viable cells. Cell viability was then calculated as the ratio of viable cells to total cells. Viability was maintained above 85% for the duration of the incubation.

These cell culture practices were also used for control experiments where the control cells were not treated with DOX.

2.3. Sample preparation

Following treatment, the cells were pelleted and washed twice in STEP buffer and divided into three replicates and diluted to a final density of 10.7×10^5 cells/ml. Each replicate of the CEM/C2 and CCRF-CEM cells had a final volume of 1.0 mL and 0.71 mL, respectively. Similar volume adjustments for the various subcellular fractions are described below. Cells were disrupted by 15 strokes of a Dounce homogenizer on ice. Disruption was monitored by microscopy until greater than 95% disruption was achieved. For the control, the cell lysate was directly mixed with BS buffer. For the DOX-treated cells, the cell lysate was fractionated by differential centrifugation as described below.

The nuclear-enriched fraction (NEF) was obtained by centrifugation at 500 g for 20 min. The supernatant was removed and the remaining pellet was dissolved in BS buffer (875 μL and 650 μL for CEM/C2 and CCRF-CEM cells, respectively). The supernatant from the NEF fraction was used to obtain the heavy organelle-enriched fraction (HOEF) by centrifugation at 4000 g for 20 min. The pellet was dissolved in BS buffer (850 μL and 550 μL for CEM/C2 and CCRF-CEM cells, respectively) following removal of the supernatant. The supernatant from the HOEF was then centrifuged at 15000 g for 30 min to obtain the light organelle-enriched fraction (LOEF). Although mitochondria are likely to be present in both the HOEF and the LOEF, the HOEF was expected to have the higher mitochondrial content [24,25]. This pellet was dissolved in BS buffer (800 μL and 500 μL for CEM/C2 and CCRF-CEM cells, respectively) following removal of the supernatant. The supernatant from the LOEF was taken to be the cytosol-enriched fraction (CEF) (final volumes of the CEFs were 750 μL and 450 μL for CEM/C2 and CCRF-CEM cells, respectively). No BS buffer was added to the CEF prior to analysis since it contained the remaining soluble components of the cell.

2.4. CE-LIF analysis

Direct MEKC analysis of the fraction lysates was performed using a home-built capillary electrophoresis instru-

ment. This instrument has been described previously [26]. Separation voltage was supplied by a CZE1000R high voltage power supply (Spellman, Hauppauge, NY, USA). The 488 nm line of an argon ion laser (Melles Griot, Carlsbad, CA, USA) was used for fluorescence excitation. Data was collected at 50 Hz using a Labview (National Instruments, Austin, TX, USA) program written in house. Samples were separated under positive polarity in a 37.8 cm uncoated fused-silica capillary with an internal diameter of 50 μm and outer diameter of 150 μm. Two millimeters of the polyimide coating were burned off at each end of the capillary.

The detector was aligned by continuously injecting 10^{-9} M fluorescein and maximizing the response of the photomultiplier tube (PMT) (Hammamatsu, Bridgewater, NJ, USA) by adjusting the position of the cuvette with x, y, and z translation stages. Samples were injected hydrodynamically for 3.5 s at 2.6 kPa and then separated under +400 V/cm. Hydrodynamic injection was used to prevent electrokinetic bias during sampling. Electrophoresis running buffer was BS buffer. Fluorescence detection was done using a post-column sheath flow cuvette with a 635 ± 27.5 nm bandpass filter (Omega Optical, Brattleboro, VT, USA). A PMT biased at 1000 V was used to collect the fluorescence. In order to minimize migration time and peak area variations between injections during electrophoresis, the capillary was reconditioned by flushing it consecutively with water, 0.1 M HCl, water, 0.1 M NaOH, water, and BS buffer for two minutes each. A constant pressure of 110 kPa was applied via a buffer pressurizing chamber. The capillary was stored in running buffer between analyses.

2.5. Data analysis

Data were smoothed with a 10 point Median Filter and 10 point binomial smoothing in the Igor Pro (Wavemetrics, Lake Oswego, OR, USA). In order to estimate the amount of DOX (or metabolites) in each fraction, a calibration curve based on DOX peak area (X) versus DOX molar concentration (Y) was constructed with DOX standards. The logarithmic equation $y = (0.456 \pm 0.016)\ln(X) - (8.77 \pm 0.03)$ fit the data from the concentration range of 1×10^{-10} to 1×10^{-8} M DOX with $r^2 = 0.995$.

2.6. Numbering and identification of metabolites

In order to number the DOX metabolites, the observed electrophoretic mobility (μ) was calculated as $\mu = LE^{-1}t_M^{-1}$, where L is the capillary length, E the electric field, and t_M is the migration time. However, μ does not take into account run-to-run variations in electroosmotic flow or the changes in analyte partitioning between the aqueous environment and the micelles present in the separation buffer. The observed electrophoretic mobility difference (OMD) between a given metabolite and a reference peak (DOX) was therefore also calculated since this parameter is better suited for metabolite identification purposes when the electroosmotic flow is not constant from run to run. The observed mobility ratio (OMR), which is determined by dividing the observed electrophoretic mobility (OM) of the metabolite by the observed electrophoretic mobility of DOX, was also calculated since it is generally believed that systematic alterations in partitioning between the aqueous and micellar phase may be reduced when this parameter is used. Similar correction procedures have previously resulted in an improvement in migration time and electrophoretic mobility reproducibilities [27–32].

In order to determine if 7-deoxyDOXone was present in the subcellular fractions, we spiked the NEFs of the two cell lines with 5×10^{-8} M of this standard. Similary, to determine if DOXone was present in the subcellular fractions, we spiked the NEFs of the two cell lines with 1×10^{-8} of this standard. After addition of the metabolite standard, the spiked fraction was analyzed and compared to the un-spiked NEF. The tentative identification of a metabolite was based on (i) the OMR of the spiked metabolite and the OMR of the un-spiked sample, and on (ii) the increase in peak intensity after spiking.

2.7. Statistical analysis

One tailed *t*-test assuming equal variances was performed using a Microsoft Excel spreadsheet. A *t*-test was performed on the OMR values of all adjacent peaks to determine if the means of the two sets of OMR values tested were statistically the same. For all *t*-tests, the null hypothesis "there is no difference in the means of the OMR values" was tested at a confidence interval (P) of 0.05. The null hypothesis was rejected when $P < 0.05$.

3. Results and discussion

3.1. Metabolite separation

In order to eliminate losses or bias due to the extraction procedure, we directly treated the subcellular fractions with the BS separation buffer. The presence of 10 mM S.D.S in this buffer facilitates the disruption of subcellular structures, solubilizes DOX metabolites, and establishes a pseudostationary phase in which DOX and its metabolites partition. The high pH of this buffer (pH 9.3) helps decrease the risk of losing DOX or its metabolites to the capillary walls [33] because, at this pH, DOX and its metabolites, as well as the capillary walls, are expected to have a net negative charge. Fig. 1 shows a representative electropherogram of a nuclear-enriched fraction of DOX-treated CEM/C2 cells (Trace A) and CCRF-CEM cells (Trace B). For the control, (i.e. solubilized lysate from untreated cells), the corresponding electropherogram did not have any peaks in the 200–290 s migration time region, where metabolites were expected to appear (Data not shown). The absence of peaks in this region of the control suggests that naturally

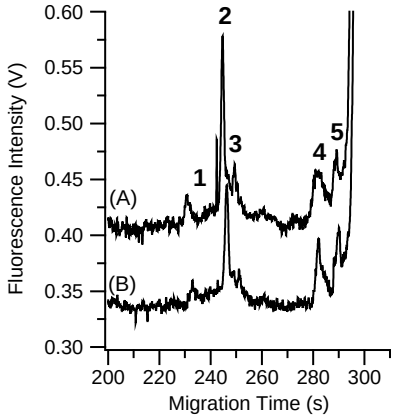

Fig. 1. Representative Electropherogram of NEF. MEKC analysis of the nuclear-enriched fraction of DOX-treated CEM/C2 cells (A) and DOX-treated CCRF-CEM cells (B). Treatment: 10 μM DOX for 12 h. The metabolite numbering system has been indicated above trace A. Separation was performed in 43.2 cm uncoated capillary at +400 V/cm following a 3.5 s hydrodynamic injection at 2.7 kPa. BS buffer was used as the running buffer and sample buffer. The 488 nm line of an argon-ion laser was used for excitation and a 635 ± 27.5 nm band-pass filter was used for detection. Traces have been offset for clarity.

fluorescent compounds that may be present in these cells were not detectable (c.f. Fig. 1).

Fig. 1 also provides the numbering system of the five metabolites that were identified in the various subcellular fractions. We initially attempted to assign metabolite numbers based on the observed electrophoretic mobility (Fig. 2, black bars), but this assignment was not straightforward because of high relative standard deviations within replicates. Such variations are to be expected when complex biological matrices (e.g. cell lysates or subcellular fractions) are directly analyzed by MEKC because the matrix components may adhere to the capillary wall, altering the electroosmotic flow, or may alter the micellar equilibrium in the separation system [32]. Another approach that is useful for numbering metabolites takes advantage of the observed mobility difference (OMD) between a given metabolite and an internal standard (e.g. DOX). This approach is particularly useful when there are run-to-run variations in electroosmotic flow. However, using the OMD did not improve reproducibility in replicates of the same fraction (Fig. 2, light gray bars) suggesting that other factors were contributing to the observed electrophoretic mobility variations. Finally, determining the ratio between the observed mobilities of a metabolite with respect to DOX (OMR) produced the lowest relative standard deviation (Fig. 2, dark gray bars). Considering that EOF and micellar partitioning may vary in MEKC, the improvements observed with OMR comparisons suggest that the various metabolites may have been experiencing similar variations in micellar partitioning from run to run. These variations may be the result of the complex sample matrix whose components may also be interacting with the micelles.

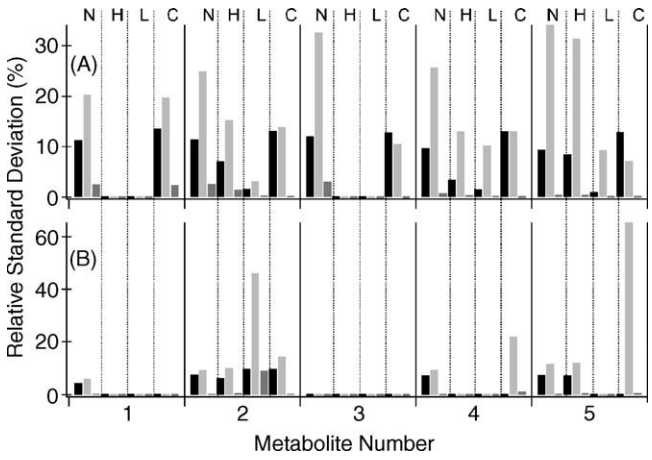

Fig. 2. Relative Standard Deviation of mobility-related parameters. The parameters for CEM/C2 cells (A), and CCRF-CEM cells (B) are: observed mobility (OM) (black), observed mobility difference (OMD) (light gray) and observed mobility ratio (OMR) (dark gray). The *x*-axis refers to the metabolite numbering system used in Fig. 1. The subcellular fractions are N: nuclear-enriched fraction; H: heavy organelle-enriched fraction; L: light organelle-enriched fraction; C: cytosol-enriched fraction. Electrophoretic mobility values were calculated as described in the Experimental section.

The OMR values for the metabolites detected in each subcellular fraction are shown in Table 1. These OMR values alone are not sufficient for assigning a metabolite number (c.f. Fig. 1) to all the metabolites in each analyzed subcellular fraction because some of these values are statistically different. For instance, OMR values for metabolites 2 and 3 for CEM/C2 cells overlap in the NEF. When the OMR is considered unreliable, other factors such as the order of metabolite migration and the general peak shape need to be taken into account when assigning tentative numbers to the detected metabolites.

As previously done by other investigators [34,35], we used synthetic standards to spike subcellular fractions and improve the tentative identification of two metabolites. Using a 7-deoxyDOXone standard, we determined that this metabolite co-migrates with metabolite 4 (Fig. 3). The average OMR of metabolite 4 in the CEM/C2 and CCRF-CEM cells (1.04 ± 0.01 and 1.05 ± 0.02, respectively, Table 1) was compared to the OMR of 7-deoxyDOXone (1.06). In both the CEM/C2 and CCRF-CEM cells, the results of the *t*-test revealed that there was no difference between the OMR of metabolite 4 and that of 7-deoxyDOXone ($P = 0.13$ and 0.34 for CEM/C2 and CCRF-CEM cells, respectively). The next closest metabolite with an average OMR value similar to that of 7-deoxyDOXone is metabolite 5 (OMR = 1.02 ± 0.01 and 1.03 ± 0.01 for CEM/C2 and CCRF-CEM cells, respectively). The OMR of metabolite 5 was also compared to that of 7-deoxyDOXone. The results of the *t*-test ($P = 0.00011$ and 0.032 for CEM/C2 and CCRF-CEM cells, respectively) indicate that there is a statistically significant difference between the OMR of metabolite 5 in both cell lines and the OMR of 7-deoxyDOXone. Therefore, taking into consideration the statistical comparison of the OMRs for metabolites 4 and 5 with the 7-deoxyDOXone standard as well as the overall

Table 1
Observed Mobility Ratio[a]

Metabolite		NEF	HOEF	LOEF	CEF	Average ± S.D.[b]	R.S.D. (%)
1	CEM/C2	1.26 ± 0.03	ND	ND	1.21 ± 0.03	1.24 ± 0.04 ($n = 6$)	3.0
	CCRF-CEM	1.29 ± 0.01	ND	ND	ND	1.29 ± 0.01 ($n = 2$)	0.51
2	CEM/C2	1.18 ± 0.03	1.18 ± 0.02	1.187 ± 0.004	1.168 ± 0.003	1.18 ± 0.02 ($n = 12$)	1.5
	CCRF-CEM	1.22 ± 0.01	1.21 ± 0.01	1.25 ± 0.1	1.17 ± 0.01	1.21 ± 0.06 ($n = 12$)	4.8
3	CEM/C2	1.15 ± 0.04	ND	ND	1.13 ± NA[c]	1.14 ± 0.03 ($n = 4$)	2.6
	CCRF-CEM	ND	ND	ND	ND	–	–
4	CEM/C2	1.05 ± 0.01	1.047 ± 0.005	1.026 ± 0.003	1.057 ± 0.001	1.04 ± 0.01 ($n = 11$)	1.2
	CCRF-CEM	1.065 ± 0.002	ND	1.01[c]	1.05 ± 0.02	1.05 ± 0.02 ($n = 7$)	2.0
5	CEM/C2	1.02 ± 0.01	1.02 ± 0.01	1.02 ± 0.002	1.029 ± 0.002	1.02 ± 0.01 ($n = 10$)	0.6
	CCRF-CEM	1.035 ± 0.002	1.04 ± 0.01	ND	1.01 ± 0.01	1.03 ± 0.01 ($n = 7$)	1.2

ND: not detected; S.D.: standard deviation; R.S.D.: relative standard deviation. NEF: nuclear-enriched fraction. HOEF: heavy organelle-enriched fraction. LOEF: light organelle-enriched fraction. CEF: cytosol-enriched fraction.

[a] Observed mobility ratio (OMR) is calculated using the ratio of observed mobilities for a given metabolite to DOX mobility. Average OMR values were calculated based on triplicate determinations.

[b] The OMR values for each metabolite from all fractions were pooled; the "Average ± S.D." column reflects the overall average and standard deviation of these pooled OMR. The number of values used to calculate the overall average and standard deviation (n) is shown in the table.

[c] Value is the result of one determination; therefore, no standard deviation was calculated.

peak profiles, we can tentatively identify Metabolite 4 as 7-deoxyDOXone.

In a separate experiment, DOXone standard was added to a different NEF extract (Fig. 4). None of the metabolite peaks co-migrated with the DOXone standard, indicating that DOXone was not present at a detectable level in any of the subcellular samples. It is important to note that the OMR of DOXone (1.13) alone is not sufficient for negating the presence of this metabolite since this value does overlap with the OMR of the nearest metabolite, Metabolite 3 (1.14 ± 0.03), in the sample. The co-migration experiment and the order in which metabolites appear in the electropherogram allowed us to conclude that Metabolite 3 is not DOXone.

Due to the lack of additional metabolite standards, the tentative identification of metabolites 1, 2, 3, and 5 was not carried out. Further identification experiments based on mass spectrometry are in progress.

3.2. Subcellular distribution of DOX metabolites

A summary of the concentrations of the fluorescent DOX metabolites separated by MEKC and detected by LIF in the subcellular fractions from CEM/C2 cells and CCRF-CEM cells is shown in Fig. 5A and B, respectively. In order to estimate the concentration of each metabolite, it was assumed that the LIF detector response for each metabolite was the same as for DOX. The concentrations for each metabolite were then determined using the calibration curve described in the Experimental section. Besides the variation in concentration observed for each of the metabolites in each subcellular fraction, the DOX concentration was about two orders of magnitude higher (see right y-axis in Fig. 5).

In order to eliminate the dilution effect that occurs when metabolites found in subfemtoliter- to picoliter-volume subcellular compartments are dissolved into the microliter-

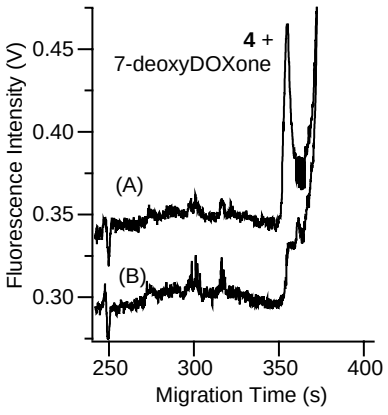

Fig. 3. Tentative identification of 7-deoxyDOXone by co-migration with standards. MEKC analysis of the nuclear-enriched fraction from CCRF-CEM cells treated with 10 μM DOX for 12 h (B). The same sample spiked with 5×10^{-9} M 7-deoxyDOXone and co-migrated with metabolite 4 (A). Separation was performed in an 37.3 cm uncoated capillary using the conditions described in Fig. 1. Traces have been offset for clarity.

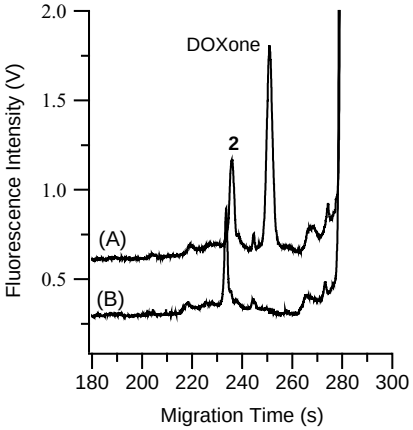

Fig. 4. Ruling out the presence of DOXone by co-migration with standards. MEKC analysis of the nuclear-enriched fraction from CEM/C2 cells treated with 10 μM DOX for 12 h (B). The same sample spiked with 1×10^{-8} M DOXone (A). Metabolite 2 is shown as a reference. Separation conditions are described in Fig. 1. Traces have been offset for clarity.

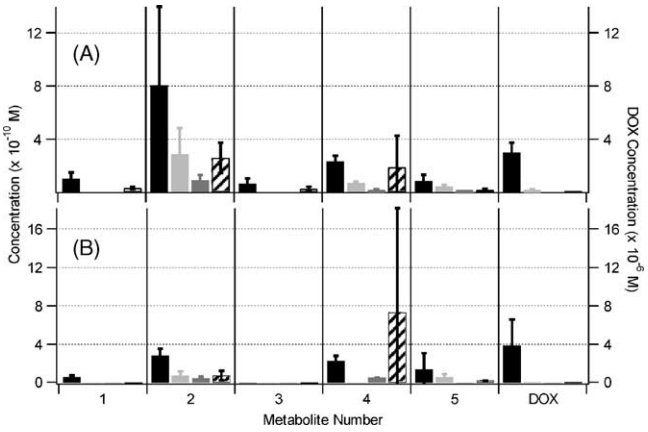

Fig. 5. Metabolite Distribution in Subcellular Fractions. In CEM/C2 cell (A) and CCRF-CEM (B), the concentrations of five metabolites were calculated from their peak areas in the electropherogram of four subcellular fractions: NEF (black), HOEF (light gray), LOEF (dark gray), CEF (diagonal fill). The *x*-axis refers to the metabolite numbering system used in Fig. 1. Error bars correspond to the standard deviation in the calculated concentrations of three independent sample preparations.

volumes of the subcellular fractions, we determined the relative abundance of these metabolites with respect to DOX. The relative abundances of these metabolites in each subcellular fraction were calculated from their peak areas in the corresponding electropherograms (Table 2). The differences in metabolite accumulation and abundance likely result from the biochemical differences between the CEM/C2 and CCRF-CEM cells. However, at the present time it is not clear how DOX metabolism is related to a reduction in topoisomerase I activity in the CEM/C2 cells, a reduction that does not occur in the CCRF-CEM cell line [22]. The very weak cross-resistance to DOX displayed by the CEM/C2 cell line is in keeping with the lack of molecular interactions between DOX and topoisomerase 1. However, DOX metabolism is believed to be mainly controlled by cytosolic enzymes [6]. In addition, it cannot be ruled out that, since the CEM/C2 have a slower growth pattern than the CCRF-CEM cells, the observed metabolite accumulation difference in the two lines may result from differences in their respective cell division times. A summary of the salient differences in the observed subcellular metabolite profiles follows.

3.2.1. Metabolite 1

The most striking feature of this metabolite is that it is only detected in the NEF samples of both the CEM/C2 cells and the CCRF-CEM cells, and in the CEF of the CEM/C2 cell line. The absence of this metabolite in the organelle fractions (HOEF and LOEF) suggests that metabolite 1 may be in fact part of a molecular complex that is not capable of partitioning or translocating into mitochondria or acidic organelles.

3.2.2. Metabolite 2

This metabolite was detected in all four subcellular fractions in both cell lines and was present at the highest concentration of any of the metabolites in the CEM/C2 cells (Fig. 5A). The highest concentration in the nuclear-enriched fraction (Fig. 5) seems to stem from the large volume fraction that the nucleus occupies within the cell. On the other hand, the LOEF has the highest relative abundance of metabolite 2 in both cell lines (Table 2). The higher organellar and cytoplasmic relative abundance indicates that metabolite 2 may be involved in cytotoxicity related to the mitochondria or plasma membrane.

3.2.3. Metabolite 3

Similarly to metabolite 1, metabolite 3 was only detected at low abundance in the NEF and CEF of the CEM/C2 cells (c.f. Table 2, Fig. 5A). Metabolite 3 was not detected at

Table 2
Relative Abundance[a] of Metabolites in CEM/C2 and CCRF-CEM cells

Metabolite		NEF	HOEF	LOEF	CEF
1	CEM/C2	0.005 ± 0.001	–	–	0.05 ± 0.02
	CCRF-CEM	0.004 ± 0.004	–	–	–
2	CEM/C2	0.04 ± 0.02	0.3 ± 0.1	0.7 ± 0.6	0.34 ± 0.05
	CCRF-CEM	0.02 ± 0.01	0.15 ± 0.05	1.1 ± 0.9	0.20 ± 0.06
3	CEM/C2	0.004 ± 0.001	–	–	0.04 ± 0.01
	CCRF-CEM	–	–	–	–
4	CEM/C2	0.012 ± 0.001	0.10 ± 0.09	0.13 ± 0.07	0.2 ± 0.2
	CCRF-CEM	0.01 ± 0.01	–	2[b]	2 ± 2
5	CEM/C2	0.005 ± 0.001	0.03 ± 0.01	0.07 ± 0.05	0.04 ± 0.02
	CCRF-CEM	0.01 ± 0.02	0.1 ± 0.1	–	0.08 ± 0.04
TA[c]	CEM/C2	0.07 ± 0.02	0.4 ± 0.1	0.9 ± 0.6	0.7 ± 0.2
TA[c]	CCRF-CEM	0.04 ± 0.02	0.2 ± 0.1	3.1 ± 0.9	2 ± 2

[a] Relative abundance was calculated with respect to the DOX peak area in the same subcellular fraction and expressed as percentage.
[b] Value is the result of one determination therefore no standard deviation was calculated.
[c] The total abundance of metabolites (TA) for each fraction and total metabolite abundance (TM) for all fractions are indicated at the bottom row. Other abbreviations are described in Table 1.

all in CCRF-CEM cells (c.f. Table 2, Fig. 5B). Due to its relatively low abundance, it is unlikely that metabolite 3 is involved in cellular toxicity.

3.2.4. Metabolite 4 (7-deoxyDOXone)

The detection of this metabolite in almost all the subcellular fractions, except for the heavy organelle enriched fraction of the CCRF-CEM cell line, implies that this metabolite is either produced in various subcellular environments, or is produced in a single subcellular environment and redistributed after production (c.f. Table 2, Fig. 5). In addition, this metabolite seems to be the most abundant metabolite in the CCRF-CEM cell line (c.f. Fig. 5B). If this metabolite is indeed 7-deoxyDOXone, then the production of this metabolite in the cytoplasm as suggested by Licata et al. [6] may be followed by partitioning and distribution to other subcellular regions. If the metabolite reaches the mitochondria at this point, it may then have cytotoxic effects as discussed by Sokolove [5]. However, since 7-deoxyDOXone was not detectable in the organelle fraction containing most of the mitochondria (HOEF) of the CCRF-CEM cell line (Fig. 5B), cytotoxicity may not be an issue in this line.

3.2.5. Metabolite 5

This metabolite was detected in all four subcellular fractions except for the LOEF of the CCRF-CEM cells (c.f. Table 2, Fig. 5). Given that its mobility is close to that of DOX (i.e. OMR $\approx$ 1), metabolite 5 may be highly similar to DOX in structure. We know that this metabolite is not DOXol because we found out previously that doxorubicinol co-migrates with DOX in MEKC separations carried out in BS buffer [19].

3.2.6. Doxorubicin

DOX concentration was noticeably higher in the NEF of both cell lines when compared with DOX concentrations in the other subcellular fractions. DOX is also found in the HOEF at slightly higher concentrations than in the CEF and the LOEF. This result is also in agreement with the literature reports of DOX interaction with mitochondria [3,36]. The DOX presence in the CEF could be attributed to DOX interaction with the plasma membrane or to DOX transport throughout the cell. As reported previously, since the MEKC system used here does not resolve DOX from doxorubicinol [19], the reported amount of DOX represents both DOX and doxorubicinol.

4. Conclusions

In this report, we have demonstrated the use of MEKC with CE-LIF detection to create metabolite profiles of DOX and five of its metabolites from four enriched subcellular fractions of CEM/C2 and CCRF-CEM cell lysates. One metabolite (metabolite 4) was tentatively identified as 7-deoxyDOXone by comparing its OMR with that of a pure standard and by co-migration with that standard. The relative abundances of metabolites with respect to DOX clearly indicate differences in metabolite accumulation between cell lines and among subcellular fractions. The concentration of a metabolite in a given subcellular fraction indicates the potential role that the metabolite may play that subcellular environment. Ultimately, the identification of all the metabolites by techniques such as mass spectrometry and the improved purification of subcellular fractions may further unveil the complexities of subcellular distribution and DOX metabolism, two key features of drug resistance, sensitivity, and cytotoxicity.

Acknowledgements

This work was supported by NIH R01-GM61969. We thank Dr. A. Suarato (Pharmacia, Nerviano, Italy) for kindly donating the doxorubicin and doxorubicinol standards used in this research and Angie Eder for critically revising this manuscript.

References

[1] G.N. Hortobagyi, Drugs 54 (1997) 1.
[2] D.J. Booser, G.N. Hortobagyi, Drugs 47 (1994) 223.
[3] R. Jeyaseelan, C. Poizat, H. Wu, L. Kedes, J. Biol. Chem. 272 (1997) 5828.
[4] L.E. Solem, L.J. Heller, K.B. Wallace, J. Mol. Cell. Cardiol. 28 (1996) 1023.
[5] P.M. Sokolove, Int. J. Biochem. 26 (12) (1994) 1341.
[6] S. Licata, A. Saponiero, A. Mordente, G. Minotti, Chem. Res. Toxicol. 13 (2000) 414.
[7] A. Bodley, L.F. Liu, M. Isreal, R. Seshadri, Y. Koseki, F.C. Giuliani, S. Kirschenbaum, R. Silber, M. Potmesil, Cancer Res. 49 (1989) 5969.
[8] K. Barabas, J.A. Sizensky, W.P. Faulk, The Journal of Biological Chemistry 267 (1992) 9437.
[9] P.M. Sokolove, FEBS Letters 234 (1988) 199.
[10] P.M. Sokolove, Arch. Biochem. Biophys. 284 (1991) 292.
[11] K.K. Singh, J. Russell, B. Sigala, Y.G. Zhang, J. Williams, K.F. Keshav, Oncogene 18 (1999) 6641.
[12] E. Goormaghitgh, P. Huart, R. Brasseur, J.M. Ruysschaert, Biochim. Biophys. Acta 861 (1986) 83.
[13] L.C. Papadopoulou, G. Theophilidis, G.N. Thomopoulos, A.S. Tsiftsoglou, Biochemical Pharmacology 57 (1999) 481.
[14] Y.P. Hu, C.T. Moraes, N. Savaraj, W. Priebe, T.J. Lampidis, Biochem. Pharmacol. 60 (2000) 1897.
[15] N. Altan, Y. Chen, M. Schindler, S.M. Simon, J. Exp. Med. 187 (1998) 1583.
[16] J. van Asperen, O. van Tellingen, J.H. Beijnen, J. Chromatogr. B 712 (1998) 129.
[17] P. Zhao, A.K. Dash, J. Pharm. Biomed. Anal. 20 (1999) 543.
[18] P.W. Buehler, S.J. Robles, G.R. Adami, R. Gajee, A. Negrusz, Chromatographia 49 (1999) 557.
[19] A.B. Anderson, J. Gergen, E.A. Arriaga, J. Chromagr. B 769 (2002) 97.
[20] A. Anderson, C.M. Ciriacks, K.M. Fuller, E.A. Arriaga, Anal. Chem. 75 (2003) 8.

[21] N. Simeon, E. Chatelut, P. Canal, M. Nertz, F. Couderc, J. Chromatogr. A 853 (1999) 449.
[22] R. Kapoor, D.L. Slade, A. Fujimori, Y. Pommier, W.G. Harker, Oncol. Res. 7 (1995) 83.
[23] A. Fujimori, W.G. Harker, G. Kohlhagen, Y. Hoki, Y. Pommier, Cancer Res. 55 (1995) 1339.
[24] J. Meijer, A. Bergstrand, J.W. DePierre, Biochem. Pharmacol. 36 (1987) 1136.
[25] C.J. Glover, K.D. Hartman, R.L. Felstad, J. Biol. Chem. 272 (1997) 28680.
[26] C.F. Duffy, S. Gafoor, D. Richards, H. Ahmadzadeh, R. O'Kennedy, E.A. Arriaga, Anal. Chem. 73 (2001) 1855.
[27] N. Chen, S. Terabe, T. Nakagawa, Electrophoresis 16 (1995) 1457.
[28] F. Tagliaro, F.P. Smith, S. Turrina, V. Equisetto, M. Marigo, J. Chromatogr. A 735 (1996) 227.
[29] M. Azad, C. Silverio, Y. Zhang, V. Villareal, F.A. Gomez, J. Chromatogr. A 1027 (2004) 193.
[30] D. Liang, J. Zhang, B. Chu, Electrophoresis 24 (2003) 3348.
[31] T. Sokoliess, M. Gronau, U. Menyes, U. Roth, T. Jira, Electrophoresis 24 (2003) 1648.
[32] C.M. Boone, J.P. Franke, R.A. de Zeeuw, K. Ensing, J. Chromatogr. A 838 (1999) 259.
[33] J. de Jong, A. Bast, W.J.F. van der Vijgh, Trends Anal. Chem 12 (1993) 422.
[34] G. Hempel, P. Schulze-Westhoff, S. Flege, N. Laubrock, J. Boos, Electrophoresis 19 (1998) 2939.
[35] L. Alvarez-Cedron, M.L. Sayalero, J.M. Lanao, Journal of Chromatography B 721 (1999) 271.
[36] E. Goormaghitgh, P. Chatelain, J. Caspers, J.M. Ruysschaert, Biochim. Biophys. Acta 29 (1980) 3003.